ISSN 1392-1207. MECHANIKA. Vol. 31, No. 4, 2025: 404–409

Motion Control of AUV Vertical Plane Based on RBF Neural Network Backstepping Sliding Mode

Mu LI*,, Ming PANG***, Guangyu CHANG******

**School of Aeronautical Engineering, Jilin University of Chemical Technology, Changchun 132022, China*
***Jitian Xingzhou (Changchun) Aerospace Technology Co., Ltd, Changchun 130000, China*
****College of Intelligent Systems Science and Engineering, Harbin Engineering University, Harbin 150001, China*
*****Institute of Robotics and Intelligent Systems, Dalian University of Technology, Dalian 116024, China,*
E-mail: l1ghty@163.com (Corresponding Author)

https://doi.org/10.5755/j02.mech.42015

1. Introduction

The ocean contains countless minerals and energy, exploration and research of marine areas have become an important task. However, it is difficult for humans to infiltrate extreme environments such as higher depths or dangerous areas [1-3]. In such case, autonomous underwater vehicle (AUV) as an advanced underwater detection robot, plays a vital role for such tasks nowadays. Generally, AUV needs to dive to a specified depth to perform exploration tasks, so research on AUV depth control has practical engineering significance [4-9].

AUV is a highly nonlinear system with strong coupling, and the hydrodynamic derivatives are difficult to accurately estimate. Therefore, AUV cannot be effectively controlled by traditional linear control methods. In addition, unpredictable disturbances may have a significant impact on the entire system, which increases the difficulty of controller design [10-13]. Aiming at the pitch control problem of AUV, Paper [11] presented a cascade PID controller which was simple to implement and had strong flexibility, but lack of self-adaptive ability. An adaptive fuzzy PID controller was proposed in [11], which can improve PID parameters and modeling uncertainty of AUV. A neural network-based adaptive controller was proposed in [12], a portion of the unknown dynamics of AUV was approximated by neural networks. Paper [13] employed radial basis functions (RBF) to address model uncertainties while incorporating prescribed performance functions with backstepping control. An adaptive control law was developed based on Lyapunov stability theory and applied to AUV control, with simulation results validating the method's effectiveness.

In this paper, an RBF neural network backstepping sliding mode control (RBFNN-BSSMC) algorithm is proposed, under the condition that the external perturbation is considered and the parameters in the AUV model are uncertain. The proposed method integrates three key innovations:

Hybrid Control Architecture: The proposed method combines backstepping control (for systematic stability guarantees), sliding-mode control (for robustness against disturbances), and RBF neural networks (for adaptive parameter estimation). This three-fold integration addresses both parametric uncertainties and unmodeled dynamics comprehensively.

Multi-RBFNN Adaptive Laws: Unlike conventional schemes that rely on a single network to approximate system dynamics, the proposed method employs multiple networks for more comprehensive fitting and higher approximation accuracy.

Stability Analysis: System stability is rigorously proven via Lyapunov theory, explicitly accounting for neural-network approximation errors—a critical feature often overlooked in conventional controllers.

Firstly, the vertical plane motion equation of the AUV is established by the analysis of the equation with six degrees of freedom (6-DOF), then the backstepping sliding mode controller is designed according to the second method of Lyapunov. In addition, the structure and algorithm of the RBFNN are briefly introduced, the adaptive laws of the multiple RBF networks are designed. Finally, the depth tracking and error curve are obtained through the simulation, which proves the availability of the control method design.

2. AUV Dynamic Model

To describe the AUV maneuvering motion, it is customary to establish a fixed coordinate system and a moving coordinate system, where the center of gravity and buoyancy are both on the same vertical line, and the origin of the moving coordinate system coincides with the center of gravity.

Through the kinematics and dynamics analysis of the AUV, the 6-DOF motion equation of the AUV is established:

$$\boldsymbol{M}\dot{\boldsymbol{\upsilon}}+\boldsymbol{C}(\boldsymbol{\upsilon})\boldsymbol{\upsilon}+\boldsymbol{D}(\boldsymbol{\upsilon})\boldsymbol{\upsilon}+\boldsymbol{g}(\boldsymbol{\eta})=\boldsymbol{\tau}, \tag{1}$$

$$\dot{\boldsymbol{\eta}}=\boldsymbol{J}(\boldsymbol{\eta})\boldsymbol{\upsilon}, \tag{2}$$

$$\dot{\boldsymbol{\eta}}=\begin{bmatrix}\dot{x} & \dot{y} & \dot{z} & \dot{\varphi} & \dot{\theta} & \dot{\psi}\end{bmatrix}^T, \tag{3}$$

$$\boldsymbol{\upsilon}=\begin{bmatrix}u & v & w & p & q & r\end{bmatrix}^T, \tag{4}$$

where $\boldsymbol{M}$ is the inertia matrix, $\boldsymbol{C}(\boldsymbol{\upsilon})$ is the Coriolis force and centripetal force matrix, $\boldsymbol{D}(\boldsymbol{\upsilon})$ is the damping matrix, $\boldsymbol{g}(\boldsymbol{\eta})$ is the gravitational buoyancy and moment vector, $\boldsymbol{\tau}$ is the control input vector, $\boldsymbol{J}(\boldsymbol{\eta})$ is the generalized Jacobian matrix, $\dot{\boldsymbol{\eta}}$ is the generalized velocity vector, $\boldsymbol{\upsilon}$ is the generalized velocity vector, φ, θ, ψ are the roll, pitch and yaw angle, u, v, w are the longitudinal, lateral and vertical speed, p, q, r are the roll, pitch and yaw angular velocity.

To realize the decoupling of the vertical and horizontal motion, the influence of lateral speed, roll motion and

yaw motion are not considered. On this basis, the following assumptions are adopted.

Assumption 1: u is a fixed value or changes gently.

Assumption 2: θ is small and $sin\theta \approx \theta$.

Assumption 3: w is small and can be ignored.

The dynamics equation of the AUV vertical plane motion is obtained when the above assumptions are satisfied:

$$\begin{cases} \dot{z} = -u\theta \\ \dot{\theta} = q \\ \left(I_y - M_{\dot{q}}\right)\dot{q} = \left(M_q + M_{q|q|}|q|\right)q - hG\theta + \tau \end{cases}, \tag{5}$$

where $M_{\dot{q}}$ is the additional mass, I_y is the moment of inertia, M_q, $M_{q|q|}$ are the hydrodynamic derivatives, h is the metacentric height, G is the gravity, τ is the control inputs of the AUV system.

The state equation of AUV vertical plane motion is obtained based on Eq. (5):

$$\begin{cases} \dot{z} = -u\theta \\ \dot{\theta} = q \\ \dot{q} = \dfrac{-hG}{I_y - M_{\dot{q}}}\theta + \dfrac{\left(M_q + M_{q|q|}|q|\right)}{I_y - M_{\dot{q}}}q + \dfrac{1}{I_y - M_{\dot{q}}}\tau \end{cases}. \tag{6}$$

3. Backstepping Sliding Mode Controller Design

The scheme of RBFNN-BSSMC and AUV system is shown in Fig. 1.

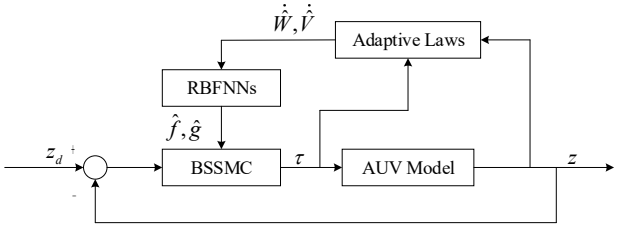

Fig. 1 Schematic of the system

Eq. (6) is simplified as follows:

$$\begin{cases} \dot{z} = -u\theta \\ \dot{\theta} = q \\ \dot{q} = f + g\tau \end{cases}, \tag{7}$$

where f, g are unknown nonlinear function.

The depth tracking error of vertical plane motion is defined as $e = z_d - z$, where z_d is the expected value of depth, the time derivative of e is indicated as below:

$$\dot{e} = \dot{z}_d - \dot{z} = \dot{z}_d + u\theta . \tag{8}$$

The Lyapunov function candidate is indicated as below:

$$V_1 = \frac{1}{2}e^2 . \tag{9}$$

The derivative of Eq. (9) is indicated as below:

$$\dot{V}_1 = e\dot{e} = e\left(\dot{z}_d - \dot{z}\right) = e\left(\dot{z}_d + u\theta\right). \tag{10}$$

To ensure that $\dot{V}_1 < 0$, Eq. (10) should satisfy that $\dot{z}_d + u\theta = -k_1 e$, where $k_1 > 0$.

The virtual control variable is designed as follows:

$$\theta_d = \frac{1}{u}\left(-\dot{z}_d - k_1 e\right). \tag{11}$$

The error of θ is defined as follows:

$$\delta = \theta_d - \theta . \tag{12}$$

The following equation is obtained by substituting Eqs. (11) and (12) into (10):

$$\dot{V}_1 = e\left(-k_1 e - u\delta\right) = -k_1 e^2 - ue\delta . \tag{13}$$

The Lyapunov function candidate is indicated as below:

$$V_2 = V_1 + \frac{1}{2}\delta^2 . \tag{14}$$

The derivative of Eq. (14) is indicated as below:

$$\dot{V}_2 = \dot{V}_1 + \delta\dot{\delta} = -k_1 e^2 + \delta\left(\dot{\delta} - ue\right). \tag{15}$$

To ensure that $\dot{V}_2 < 0$, Eq. (15) should satisfy that $\dot{\delta} - ue = -k_2\delta$, where $k_2 > 0$.

$$\dot{\delta} = \dot{\theta}_d - \dot{\theta} = \frac{1}{u}\left(-\ddot{z}_d - k_1\dot{e}\right) - q . \tag{16}$$

Then:

$$\dot{\delta} - ue = \frac{1}{u}\left(-\ddot{z}_d - k_1\dot{e}\right) - q - ue = -k_2\delta . \tag{17}$$

The virtual control variable is designed as shown below:

$$q_d = \frac{1}{u}\left(-\ddot{z}_d - k_1\dot{e}\right) - ue + k_2\delta . \tag{18}$$

The error of q is defined as follows:

$$\varepsilon = q_d - q . \tag{19}$$

Eq. (15) can be rewritten as Eq. (20) based on Eqs. (16)-(19):

$$\dot{V}_2 = -k_1 e^2 - k_2\delta^2 + \delta\varepsilon . \tag{20}$$

In this case, if $\varepsilon = 0$, then $\dot{V}_2 \le 0$. The sliding mode function is designed as $s = \varepsilon$. A new Lyapunov function candidate is as follows:

$$V_3 = V_2 + \frac{1}{2}s^2 . \tag{21}$$

The derivative of Eq. (21) is as follows:

$$\dot{s} = \dot{\varepsilon} = \frac{1}{u}\left(-\dddot{z}_d - k_1\ddot{e}\right) - u\dot{e} + k_2\dot{\delta} - \left(f + g\tau\right). \tag{22}$$

It is generally assumed that $\dddot{z}_d = 0$, in light of Eqs. (20) and (22), the time derivative of Eq. (21) is obtained:

$$\dot{V}_3 = -k_1e^2 - k_2\delta^2 + s\left(-\frac{1}{u}k_1\ddot{e} - u\dot{e} + k_2\dot{\delta} - \right.$$
$$\left. -f - g\tau + \delta\right). \tag{23}$$

To ensure that $\dot{V}_3 < 0$, an exponent approaching sliding mode controller is designed as shown below:

$$\tau = \frac{1}{g}\left[-\frac{1}{u}k_1\ddot{e} + k_2\dot{\delta} - u\dot{e} - f + \right.$$
$$\left. + ks + \xi\, sgn\left(s\right) + \delta\right], \tag{24}$$

where k, ξ are the exponential reaching law parameters.

The following equation is obtained by substituting Eq. (24) into Eq. (23):

$$\dot{V}_3 = -k_1e^2 - k_2\delta^2 - \xi\left|s\right| - ks^2 \le 0 . \tag{25}$$

In addition, to reduce the vibration, the hyperbolic tangent function *tanh* is adopted instead of the sign function *sgn*. The final backstepping sliding mode control law is obtained:

$$\tau = \frac{1}{g}\left[-\frac{1}{u}k_1\ddot{e} + k_2\dot{\delta} - u\dot{e} - f + \right.$$
$$\left. + ks + \xi\, tanh\left(s\right) + \delta\right]. \tag{26}$$

4. RBF Neural Network Design

The hydrodynamic derivatives will change with the AUV motion, which increase great uncertainty to the dynamic equations. In addition, the external perturbation, such as wave disturbance, will have a significant effect on the AUV motion. Multiple RBF networks are employed to compensate for all the unknown nonlinear functions in the dynamic equations considering the characteristics of approximating any nonlinear function.

The RBFNN was first proposed in 1988. In comparison to the feedforward BP neural network, the RBFNN has a simple structure and a high convergence speed, in addition, it is suitable for real-time control and can effectively improve the adaptability and robustness of the system [14].

The RBFNN is composed of three-layer networks, as shown in Fig. 2.

In Fig. 2, $\boldsymbol{x} = \left[x_1 \quad x_2 \quad \cdots \quad x_n\right]^T$ is the input of the RBFNN, h_j is the output of the j-th Gaussian basis function:

$$h_j = exp\left(\frac{\left\|\boldsymbol{x} - \boldsymbol{c}_j\right\|^2}{2b_j^2}\right), j = 1,2,\cdots,m , \tag{27}$$

where $\boldsymbol{c}_j = \left[c_{1j} \quad c_{2j} \quad \cdots \quad c_{nj}\right]^T$ is the center vector of the j-th Gaussian basis function, b_j is the width of the j-th Gaussian basis function.

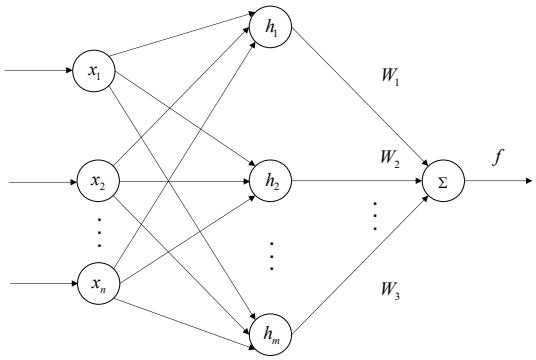

Fig. 2 Topology of RBFNN

The weight vector of RBFNN can be written as $\boldsymbol{W} = \left[W_1 \quad W_2 \quad \cdots \quad W_n\right]^T$, the output of the RBFNN neural network is indicated as below:

$$f = W_1h_1 + W_2h_2 + \cdots + W_mh_m . \tag{28}$$

The output algorithms of multiple RBF networks are designed as follows:

$$\begin{cases} f = \boldsymbol{W}^T\boldsymbol{h}_f + \varepsilon_f \\ g = \boldsymbol{V}^T\boldsymbol{h}_g + \varepsilon_g \end{cases}, \tag{29}$$

where f, g are the ideal networks outputs, $\boldsymbol{W}$, $\boldsymbol{V}$ are the ideal network approximation weight vectors, ε_f, ε_g are the network approximation errors.

The outputs of the RBF networks are obtained using the sliding mode functions as the inputs of networks:

$$\begin{cases} \hat{f} = \hat{\boldsymbol{W}}^T\boldsymbol{h}_f \\ \hat{g} = \hat{\boldsymbol{V}}^T\boldsymbol{h}_g \end{cases}, \tag{30}$$

where $\hat{\boldsymbol{W}}$, $\hat{\boldsymbol{V}}$ are the estimated values of $\boldsymbol{W}$ and $\boldsymbol{V}$.

The final control law is obtained by substituting Eq. (30) into Eq. (26):

$$\tau = \frac{1}{\hat{g}}\left[-\frac{1}{u}k_1\ddot{e} + k_2\dot{\delta} - u\dot{e} - \hat{f} + \right.$$
$$\left. + ks + \xi\, tanh\left(s\right) + \delta\right]. \tag{31}$$

The Lyapunov function candidate is indicated as below:

$$L = V_3 + \frac{1}{2\gamma_1}\tilde{\boldsymbol{W}}^T\tilde{\boldsymbol{W}} + \frac{1}{2\gamma_2}\tilde{\boldsymbol{V}}^T\tilde{\boldsymbol{V}} , \tag{32}$$

where $\gamma_1 > 0$, $\gamma_2 > 0$.

The time derivative of Eq. (32) is indicated as below:

$$\begin{aligned}\dot{L} = &-\tilde{\boldsymbol{W}}^T\left(s\boldsymbol{h}_f + \frac{1}{\gamma_1}\dot{\hat{\boldsymbol{W}}}\right) - \\ &-\tilde{\boldsymbol{V}}^T\left(s\boldsymbol{h}_g\tau + \frac{1}{\gamma_2}\dot{\hat{\boldsymbol{V}}}\right) - k_1e^2 - k_2\delta^2 - \\ &-ks^2 - s\xi\, tanh(s) - s\left(\varepsilon_f + \varepsilon_g\tau\right).\end{aligned} \tag{33}$$

The adaptive laws are designed as follows:

$$\begin{cases}\dot{\hat{\boldsymbol{W}}} = -\gamma_1 s\boldsymbol{h}_f \\ \dot{\hat{\boldsymbol{V}}} = -\gamma_2 s\boldsymbol{h}_g\tau\end{cases}. \tag{34}$$

The following equation is obtained by substituting Eq. (34) into Eq. (33):

$$\dot{L} = -k_1e^2 - k_2\delta^2 - ks^2 - s\left(\varepsilon_f + \varepsilon_g\tau\right) - \xi|s|. \tag{35}$$

Considering ε_f and ε_g are very small real numbers, we set $\xi \geq \left|\varepsilon_f + \varepsilon_g u\right|$, then $\dot{L} \leq 0$. When $\dot{L} \equiv 0$, $V_3 \equiv 0$, in term of the LaSalle invariance principle, when $t \to \infty$, $V_3 \to 0$.

5. Simulation and Analysis

In this section, two simulation examples are presented. The system and controller parameters are shown in Table 1.

Table 1

Parameters of AUV

Parameters	Values
m, kg	50
I_y, kg·m^2	8.89
$M_{\dot{q}}$	-5.97
M_q	-26.14
$M_{q\|q\|}$	-4.28
k_1	3
k_2	100
k	0.01
ξ	85
γ_1	100
γ_2	100
u, m / s	1

To verify the effectiveness of the proposed algorithm, a traditional sliding mode controller is designed for comparison, which $s = 6.25e + 5\dot{e} + \ddot{e}$, and the exponential reaching law is $\dot{s} = 0.01s + 2tanh(s)$.

Example 1: The perturbation of hydrodynamic derivatives is set to $10sin(0.2t) + 10cos(0.2t)$, the wave disturbance is set to zero, the desired depth is set to 10 m. The simulation results are plotted in Fig. 3 and Fig. 4. Fig. 3 shows the depth trajectory curves of AUV. Fig. 4 represents the response curves of pitch angle.

Example 2: The same perturbation of hydrodynamic derivatives and desired depth are adopted as the example 1, but the wave disturbance is set to $sin(0.2t)$. Fig. 5 and Fig. 6 depict the simulation results under the influence both of internal and external perturbation.

It can be seen from Fig. 3 and Fig. 5 that the great trajectory tracking precision of RBFNN-BSSMC without any chattering phenomenon. Furthermore, the proposed controller has shorter response time. Fig. 4 and Fig. 6 demonstrate the smoothness of the pitch angle of the proposed controller, while traditional sliding mode controller contains a larger vibration.

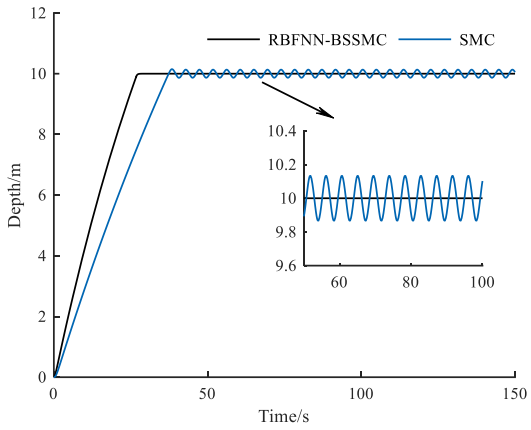

Fig. 3 Depth curves of AUV vertical plane motion

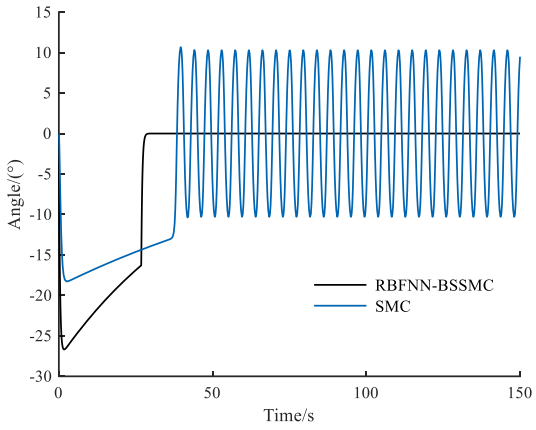

Fig. 4 Pitch angle curves of AUV

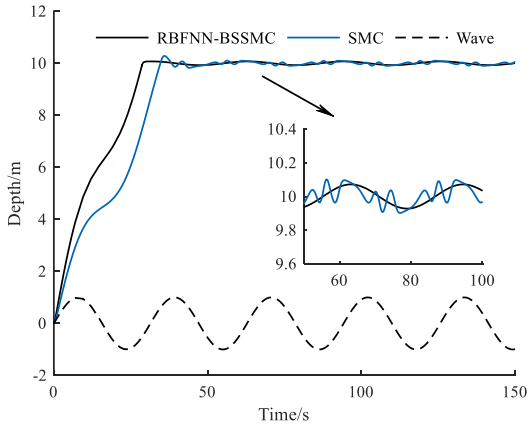

Fig. 5 Depth curves of AUV vertical plane motion

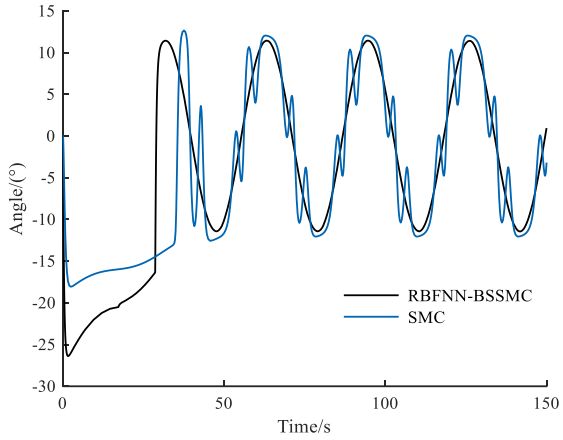

Fig. 6 Pitch angle curves of AUV

The simulation results demonstrate the promising performance and effectiveness of the proposed algorithm in terms of adaptability and robustness enhancement of the AUV system, the speed improvement of response and the chattering reduction.

6. Conclusions

In this paper, a backstepping sliding mode controller is proposed on the base of multiple RBF neural networks for AUV vertical plane motion. First, the dynamic equation of AUV vertical motion is established. Based on the state equation, a backstepping sliding mode control algorithm is developed, then the multiple RBF neural networks are adopted to compensate the modeling uncertainty and external interference. Moreover, the stability of the system is proved according to the second method of Lyapunov. The simulation results demonstrate that the designed control algorithm has better adaptability and robustness than traditional sliding mode control.

References

1. **Bessa, W. M.; Dutra, M. S.; Kreuzer E.** 2008. Depth control of remotely operated underwater vehicles using an adaptive fuzzy sliding mode controller, Robotics and Autonomous Systems 56(8): 670-677. https://doi.org/10.1016/j.robot.2007.11.004.
2. **Kang, S.; Rong, Y.; Chou, W. W.** 2020. Antidisturbance Control for AUV Trajectory Tracking Based on Fuzzy Adaptive Extended State Observer, Sensors 20(24): 7084. https://doi.org/10.3390/s20247084.
3. **Tijani, A. S.; Chemori, A.; Creuze, V.** 2022. A survey on tracking control of unmanned underwater vehicles: Experiments-based approach, Annual Reviews in Control 54: 125-147. https://doi.org/10.1016/j.arcontrol.2022.07.001.
4. **Nambisan, P. R.; Singh, S. N**. 2009. Multi-variable adaptive back-stepping control of submersibles using SDU decomposition, Ocean Engineering 36: 158-167. https://doi.org/10.1016/j.oceaneng.2008.09.011.
5. **Paull, L.; Saeedi, S.; Seto, M.; Li, H.** 2014. AUV Navigation and Localization: A Review, IEEE Journal of Oceanic Engineering 39(1): 131-149. https://doi.org/10.1109/JOE.2013.2278891.
6. **Marani, G.; Choi, S. K.; Yuh, J**. 2009. Underwater autonomous manipulation for intervention missions AUVs, Ocean Engineering 36(1): 15-23. https://doi.org/10.1016/j.oceaneng.2008.08.007.
7. **Shen, C.; Shi, Y.; Buckham, B.** 2018. Trajectory Tracking Control of an Autonomous Underwater Vehicle Using Lyapunov-Based Model Predictive Control, IEEE Transactions on Industrial Electronics 65(7): 5796-5805. https://doi.org/10.1109/TIE.2017.2779442.
8. **Borlaug, I.-L. G.; Pettersen, K. Y.; Gravdahl, J. T.** 2021. Comparison of two second-order sliding mode control algorithms for an articulated intervention AUV: Theory and experimental results, Ocean Engineering 222: 108480. https://doi.org/10.1016/j.oceaneng.2020.108480.
9. **Chen, J.; Gao, P.; Gu, H.; Chen, Y.; Xinnuo, E.; Yu J.** 2024. Experimental study of the natural deposition of submicron aerosols on the surface of a vertical circular tube with non-condensable gases, Nuclear Engineering and Design 417: 112863. https://doi.org/10.1016/j.nucengdes.2023.112863.
10. **Jianhua, W.; Yan, S.; Guoliang, W.; Bin, Y.** 2017. Application of cascade PID control in the pitch control system of a remotely operated vehicle, Journal of University of Shanghai for Science and Technology 39: 229-235. https://doi.org/10.13255/j.cnki.jusst.2017.03.005.
11. **Khodayari, M. H.; Balochian, S.** 2015. Modeling and control of autonomous underwater vehicle (AUV) in heading and depth attitude via self-adaptive fuzzy PID controller, Journal of Marine Science and Technology 20: 559-578. https://doi.org/10.1007/s00773-015-0312-7.
12. **Li, J. H.; Lee, P. M.** 2005. A neural network adaptive controller design for free-pitch-angle diving behavior of an autonomous underwater vehicle, Robotics and Autonomous Systems 52(2-3): 132-147. http://doi.org/10.1016/j.robot.2005.04.004.
13. **Wang, C.; Zhu, S.; Yu, W.; Song, L.; Guan, X.** 2021. Adaptive prescribed performance control of nonlinear asymmetric input saturated systems with application to AUVs, Journal of the Franklin Institute 358(16): 8330-8355. https://doi.org/10.1016/j.jfranklin.2021.08.026.
14. **Yang, H.; Liu, J.** 2018. An adaptive RBF neural network control method for a class of nonlinear systems, IEEE/CAA Journal of Automatica Sinica 5(2): 457-462. https://doi.org/10.1109/JAS.2017.7510820.

M. Li, M. Pang, G. Chang

MOTION CONTROL OF AUV VERTICAL PLANE BASED ON RBF NEURAL NETWORK BACKSTEPPING SLIDING MODE

S u m m a r y

Aiming at the vertical plane motion issue of autonomous underwater vehicle (AUV) with modeling uncertainty and external perturbation, a backstepping sliding mode control algorithm is proposed on the base of multiple radical basis function (RBF) neural networks. Firstly, the kinematics and dynamics equations of AUV are established. Secondly, according to the second method of Lyapunov, a robust sliding mode controller on the base of backstepping control algorithm is designed to eliminate the errors of states and improve the response speed. At the same time, multiple RBF networks are adopted to adaptively compensate for the uncertainty or nonlinear term in the AUV motion equation and external perturbation. Finally, the stability analysis for the AUV control system is given based upon the second method of Lyapunov. The simulation results demonstrate that: The presented controller can enable the AUV to reach the desired depth at a quick speed and high accuracy. In comparison to the traditional sliding mode controller, the given method possesses higher adaptability and better dynamics performance.

Keywords: autonomous underwater vehicle (AUV), backstepping control, sliding mode control (SMC), radical basis function neural network (RBFNN).

Received June 26, 2025
Accepted August 22, 2025

This article is an Open Access article distributed under the terms and conditions of the Creative Commons Attribution 4.0 (CC BY 4.0) License (http://creativecommons.org/licenses/by/4.0/).